European Journal of Therapeutics

DOI: 10.5152/EurJTher.2019.18016

Original Research

Residual Stress Levels on the Cortical Section of Vertebral Bone Tissue

Cemil Sert[1], Ayşe İmge Uslu[2], Şerife Yalçın[3]

[1]Department of Biophysics, Harran University School of Medicine, Şanlıurfa, Turkey

[2]Department of Anatomy, Sanko University School of Medicine, Gaziantep, Turkey

[3]Department of Physic, Harran University School Science, Şanlıurfa, Turkey

ABSTRACT

Objective: Residual stress can cause deformation and cracks in the bone tissue. The aim of our study is to measure the residual stress level and distribution in the cortical bone of the extremities of vertebrates.

Methods: Residual stress levels in the bone tissue of 12 sheeps aged 2 years were measured by observing the cortical parts of 6 different (C1, C3, Th1, Th 13, L1, and L6) vertebral bones by means of the X-ray diffraction method. This method is recognized as the one that can measure residual stress in the bone tissue most accurately. By means of special methods, the cortical part of vertebral bone was separated from its trabecular part. The bone tissue was left to stand for a long time to dry completely. Measurements were performed on completely dried tissues using an X-ray diffraction apparatus. The residual stress values obtained from all the subject groups were compared statistically.

Results: It was found that the residual stress level was the highest in C3 and that it showed a statistically significant change as compared to the levels in C7, Th1, and Th13. Although the level in C3 was high as compared to the levels in L1 and L6, it was not statistically significant.

Conclusion: The residual stress level in the C3 vertebral cortical section was significantly higher than other parts and was interpreted as such by us, i.e., anatomically, it is one of the vertebrae that keep the head upright and is the vertebra carrying the maximum load in all natural processes.

Keywords: Deformation, nano-cracks, residual stress, vertebral bone

INTRODUCTION

Residual stress is defined as the stress that exists in bone tissue without any external force (1, 2). Residual stress is also seen in living soft tissues, such as blood vessels (3), but primarily the existence of residual stress was has been shown in bone tissue (4). There are many physical methods used to measure residual stress, which include hole drilling, deep hole creation, sectioning method, Contour method, X-ray diffraction, ultrasonography, and the Barkhausen noise method (5). Of these methods, the X-ray diffraction method is considered to be the technique that provides the most extensive results, especially in bone tissue. Residual stress of bone tissue from the femur of cattle was measured by means of the X-ray diffraction method (6).

Cortical bone has a regular composite structure that is shaped with hydroxyapatite (HAP) minerals and collagen matrix (7-12). When the bone tissue is deformed, the distance between the lattice planes of HAP crystals shows the deformation changes in the bone tissue (10). The stress undertaken by HAP crystals can be measured by assessing the deformation in interplanar spacings and by comparing it with a reference (7, 11). Bone tissue regenerates continuously through new osteon structuring (13). New tissues develop under in-vivo loads (14, 15).

Due to non-uniform structures in the bone tissue, residual stress could be formed between changed (old and new) areas without any external force.

The purpose of this study was to measure residual stress levels in the cortical portions of the vertebral bone tissue of 12 2-year-old sheep without applying any external force, assess whether there was any difference between the stress in the cervical, thoracic, and lumbar regions, and thus find which the region with a higher probability of deformation as compared to the others. For this purpose, the first and last vertebrae of the cervical, thoracic, and lumbar regions were selected.

How to cite: Sert C, Uslu Aİ, Yalçın Ş. Residual Stress Levels on the Cortical Section of Vertebral Bone Tissue. Eur J Ther 2019; 25(4): 248–52.

ORCID IDs of the authors: C.S. 0000–0003–3894–0201; A.İ.U. 0000–0001–7375–192X; Ş.Y. 0000–0002–9791–5623

Corresponding Author: Cemil Sert **E–mail:** csert@harran.edu.tr

Received: 26.09.2018 • **Accepted:** 01.03.2019

METHODS

Separation of the Cortical Section

A total of 12 cervical vertebrae (III, IV, V, VI, and VII), 13 thoracic vertebrae, and 6 lumbar vertebrae were dissected from the sheeps' vertebral column and freed from the surrounding soft tissues. This dissected vertebrae were fixed to a table using a clamp system and bone blocks were obtained by resecting 2 mm-thick pieces from the obtained samples from the top and bottom surfaces of the corpus vertebrae using a Stryker bone cutter. All the procedures were performed by the same operator under aseptic conditions with the use of an apron, gloves, and operation glasses. The bone tissue was set out for a long time to dry it completely. Measurements were performed on completely dried tissues using the X-ray diffraction tool. Ethics committee approval is not required since this study was performed on the slaughtered sheep vertebral bone.

Residual Stress Analysis

The known methods to measure residual stress are: X-ray diffraction method, Neutron diffraction method, Barkhausen noise method, and ultrasonic method. Among these, the most reliable measurement method is accepted as the X-ray diffraction method (Methods of Measuring Residual Stresses in Components N. S. Rossinia, M. Dassistia, K. Y. Benyounisb and A. G. Olabi). For this reason, we measured all our samples using this method (5).

The residual stress value can be determined by measuring the σ and 2θ diffraction angle. The Bragg law, which is the basic method for X-ray diffraction, is given by the following equation:

$2d\sin\theta = n\lambda$

This equation establishes a relationship between the θ Bragg angle and the distance between the planes at the knowing (hkl) plane using characteristic X-rays with a monochromatic wavelength.

$\nu\theta$The values of E, ν, and θ in the formula are obtained with some operations.

E is the Young's modulus (MPa), ν is the Poisson rate, and θ is the diffraction angle in a non-stress situation.

The ψ angle between the sample surface and the lattice plane changed normally during the stress measurement, as shown in Figure 1. Detector scans to measure the intensity of X-ray were refracted by the sample.

To obtain the stress value, a graphic of the 2θ (horizontal part) and $\sin^2\psi$ (vertical part) graphic was drawn using various ψ angles. The slope of this graph is multiplied with stress constant K, which is determined by the type of material. Following this, the stress value is obtained.

Figure 1. Cortical section of Vertebral bone of 2-year-old sheep

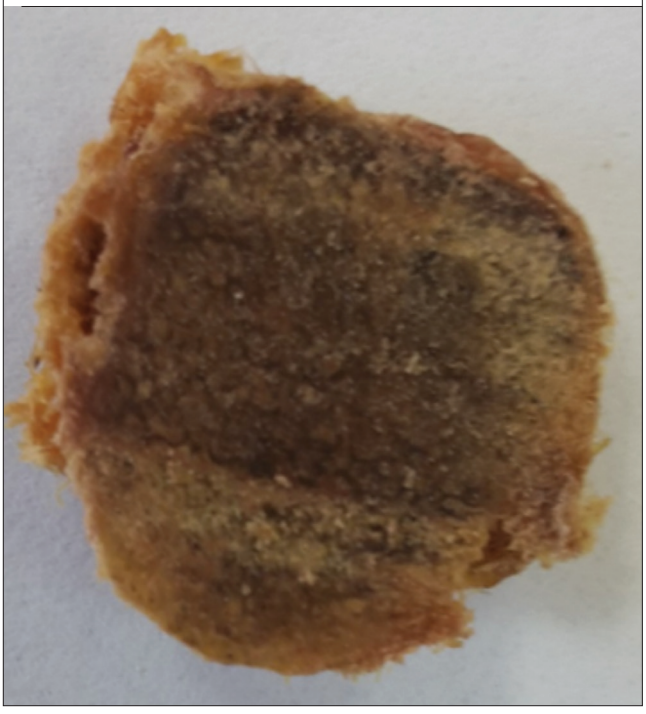

Figure 2. Residual stress measurement by X-ray refraction method

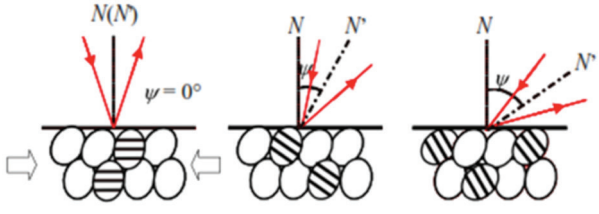

The measurements of the samples in this study were performed from up part. The measurement of residual stress by the X-ray diffraction (XRD) method is shown in Figure 2. XRD spectra were recorded by using a Rigaku X-ray diffractometer (RINT 2000 series, model D/max 2000, Rigaku Co., Japan) with a multipurpose attachment. A characteristic CuKα (l.5406 nm) X-ray source, a tube with a voltage of 40 kV, and a tube current at 40 mA was used. The incidence angle was fixed at 1° during scanning. The XRD analyzes were carried out using the symmetrical Bragg-Brentano configuration (θ-2θ) with parallel beam geometry. The diffraction profiles were measured between 10°-120°, which includes the diffraction angles of the (2 1 1), (1 1 2), and (3 0 0) lattice planes of hydroxyl apatite (HAP) crystals. The XRD peaks were found to have a hexagonal crystal structure with a P63/m (176) space group (JCPDS 98-000-0050).

The study defined 2θ as the angle at the peak position of the profile, the peak position was determined as the midpoint of the full width at half maximum intensity of the profile (FWHM method), 2θ was measured at the various ψ conditions accord-

Table 1. Mean and standard deviation of samples

	N	Mean	Standard deviation	Standard error
C3	12	4602.41	1345.33	388.36
C7	12	3320.00	595.45	171.89
Th1	12	3411.66	653.24	188.57
Th13	12	3236.58	959.19	276.89
L1	12	3688.00	1058.25	305.49
L6	12	3738.75	479.66	138.46

Table 2. Statistical results of samples of C7, Th1, Th13, L1, L6 sections are compared to C3

I group	J group	p
C3	C7	0.030
C3	Th1	0.032
C3	Th13	0.008
C3	L1	0.253
C3	L6	0.356

Figure 3. Residual stress levels of cortical section of vertebral bone tissue

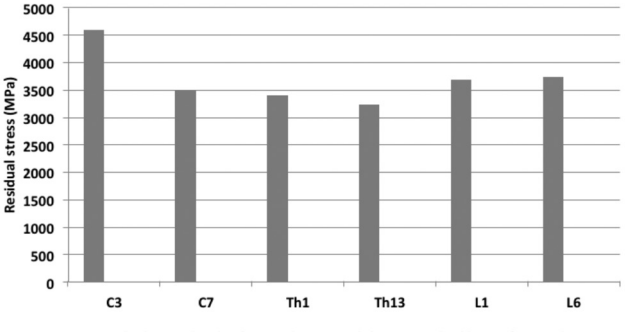

ing to the sample situation, and $q(2\theta)/q(\sin^2\psi)$ was calculated by the linear least-squares method. To determine residual stress, a residual stress calculation software was used. The samples were smoothed and the unit cell parameters of the sample obtained from the XRD pattern (a=9.364, b=9.364, c=6.881Å, alpha=90°, beta=90°, and gamma=120°) were used for residual stress calculation (Rigaku, Jade 7 software). Based on previous literature, the values of the Young's modulus and Poison rate for this sample were taken as 70 GPa and 0.3, respectively (16).

Statistical Analysis

Residual stress levels that were measured in the cortical bones C3, C7, Th1, Th13, L1 and L6 were statistically compared with each other using ANOVA oneway and Benforanni statistical methods in the Statistical Package for the Social Sciences (SPSS IBM Corp.; Armonk, NY, USA) 20 version package software (Table 1).

RESULTS

Residual stress level measurements of the cortical part of 12 sheep vertebrae were made by using the X-ray diffraction method. Residual stress levels that were measured in the cortical bones C3, C7, Th1, Th13, L1, and L6 were statistically compared with each other using the one-way analysis of variance and Benforanni statistical methods available in the SPSS version 20 software (Table 1). It was found that residual stress levels were the highest in the cortical bone of the C3 vertebra. The residual stress level of C3 showed statistically significant changes as compared to C7, L1, and L6 (C3-C7 $p<0.030$; C3-L1 $p<0.032$; C3-L6 $p< 0.008$). Results are shown in Figure 3. When compared with C3, there was a difference in the levels of Th1 and Th13 but this difference was not statistically significant (Table 2).

DISCUSSION

The value of residual stress depends on the stress constant Kx, which is calculated with the elasticity modulus Ex and the coefficient $k^*_{x'}$ which in turn, depend on HAP crystal structures, collagen fibers, and ultimately, tissue stress (10). However, the X-ray diffraction method directly measures the distribution of residual stress without using the elasticity modulus.

Yamado et al. (1) compared residual stress and osteon population density and observed a higher proportion of residual stress in areas with a high osteon population density. These results were found compatible with some past results (17, 18). However, the authors suggested that this might change depending on whether the anterior or posterior positions were sampled. This is because mineral crystal orientation could change in these regions and it does not have a direct relationship with the orientation and organization of collagen fibers (19). Yamado et al. (1) suggested that non-uniform structures of tissues are derived from osteon formation and the internal organization of these entities down to the nanostructural levels may be explained by the spatial differences in the patterns of residual stress.

Adachi et al. (20) measured residual stress in the vertebral bone by the cutting method and suggested that the bone tissue develops a stress condition to eventually become more uniform.

Residual stress might be important for mechanical strength of the tissue. Bone tissue can distribute the applied force and energy among the cells to counter daily mechanical stresses, but it may fail to distribute the same level of force after certain levels of stress, leading to the occurrence of residual stress in the tissue. This residual stress causes hair cracks in the tissue, which may easily lead to bone fragility.

Residual stress could also manifest differently in anterior and posterior positions (6). It has been shown that residual stress in the anterior position is higher than the stress seen in the posterior position in the femurs of cattle. For this reason, residual stress could be associated with energy distribution or composite distribution of the stress environment (6).

More generally, residual stress could be associated with the formation of osteon structures and/or their collagen/lamellar/crystalline organization. Some studies have also revealed a relationship between residual stress and osteon population density. However, this relationship was not found to be particularly strong.

More complex studies are needed in order to completely explain the residual stress-fragility relationship. For example, it will be necessary to examine the non-uniform distributions and collagen fiber orientation (CFO) in collagen attachments, the relationship between osteon types and/or CFO heterogeneity and residual stress, distribution of HAP crystal structures, and their orientation.

Further, residual stress may show differences in bones of different species and not only in anterior and posterior bones, since the vertebrae and other parts of the skeleton are exposed to different loads in human beings and other animals. For instance, since the cervical, thoracic, and lumbar vertebrae are loaded differently in four-footed animals, the residual stress may occur at different levels between such animals and even between different animals in the same species. For this reason, it is important to assess whether or not the residual stress levels show differences depending on different loads in cortical sections of C3, C7, Th1, Th13, L1, and L6 in adult sheep bone.

In our study, the residual stress level of C3 showed a statistically significant change as compared to C7, Th1, and Th13. A statistically insignificant difference was observed between L1 and L6, which may be due to the fact that C3 is the vertebra that carries the maximum load to support the cranium in a sheep's skeleton. Undoubtedly, this load is present at different levels in other vertebrae because all of them were found to exhibit residual stress. However, it was seen most clearly in C3 due to its anatomical structure and its maximum load-bearing position.

CONCLUSION

With the existing methods and under in-vivo conditions, it is impossible to measure whether such a difference occurs in human beings at the present time. This is because the vertebral bone would need to be isolated from the body for all these methods.

Hydroxyapatite crystal structures, lattice planes and their deformations, osteon structures, osteon population density, and deformations can provide some information about residual stresses in the bone tissue.

Ethics Committee Approval: Ethics committee approval is not required since this study was performed on the slaughtered sheep vertebral bone.

Informed Consent: N/A.

Peer-review: Externally peer-reviewed.

Author Contributions: Concept - C.S.; Design - C.S., A.İ.U.; Supervision - C.S.; Resources - C.S.; Materials - C.S., A.İ.U.; Data Collection and/or Processing - C.S., A.İ.U.; Analysis and/or Interpretation - Ş.Y., A.İ.U.; Literature Search - C.S.; Writing Manuscript - C.S., A.İ.U.

Acknowledgments: Thanks to Harran University research Fund for Financial Contributions.

Conflict of Interest: The authors have no conflicts of interest to declare.

Financial Disclosure: This work was supported by Harran University Research Funding (HÜBAK Project no: 15121).

REFERENCES

1. Yamada S, Tadano S, Fujisaki K. Residual stress distribution in rabbit limb bones. J Biomech 2001; 44: 1285-90. [CrossRef]
2. Hızal A, Sadasivam B. Residual stress in bone: A parametric study. Proceedings of IMECE 2008. ASME International Mechenical engineering Congress and Exposition. 31-09/06-10-2008; Boston, Massachusetts, USA.
3. Fung YC. Biomechanics: Motion, Flow, stress and Growth. Springer, Berlin Heidelberg. New York. USA pp. 1990. 388-3, 500-3.
4. Tadano S, Okoshi T. Residual stress in bone structure and tissue of rabbit's tibiofibula. Biomed Mater Engin 2006; 16: 11-21.
5. Rossini NS, Dassisti M, Benyounis KY, Olabi AG. Methods of measuring residual stresses in components. Materials & Design 2012; 35: 572-88. [CrossRef]
6. Yamada S, Tadano S. Residual stress around the cortical sürfece in bovine femoral diaphysis. J Biomech Eng 2010; 132: 31-4. [CrossRef]
7. Fujisaki K, Tadano S, Sasaki N. A method on strain measurement of HAp in cortical bone from diffusive profile of X-ray difraction. J Biomech 2006; 39: 379-86. [CrossRef]
8. Gupta HS, Seto J, Wagermainer W, Zaslansky P, Boesecke P, Fratzl P. Cooperative deformation of mineral and collagen in bone at the nanoscale. Proc Natl Acad Sci U S A 2006; 103: 17741-6. [CrossRef]
9. Almer JD, Stock SR. Micromechanical response of mineral and collagen phases in bone. J Struct Biol 2007; 157: 365-70. [CrossRef]
10. Fujisaki K, Tadano S. Relationship between bone tissue strain and lattice strain of HAp crystals in bovine cortical bone under tensile loading. J Biomech 2007; 40: 1832-8. [CrossRef]
11. Tadano S, Giri B, Sato T, Fujisaki K, Todoh M. Estimating nanoscale deformation in bone X-ray difraction imaging method. J Biomech 2008; 41: 945-52. [CrossRef]
12. Giri B, Tadano S, Fujisaki K, Sasaki N. Deformation of crystal in cortical bone depending on structural anisotropy. Bone 2009; 44: 1111-20. [CrossRef]
13. Currey JD. Bones: Structures and Mechanics. Princeton University Press, USA, 2002; pp.14-21.
14. Gibson VA, Stover SM, Gibeling JC, Hazelwood SJ, Martin RB. Osteonal effects on elastic modulus and fatigue life in equine bone. J Biomech 2006; 39: 217-25. [CrossRef]
15. Rho JY, Zioupos P, Currey JD, Pharr GM. Variations in the individual thick lamellar properties within osteons by nanoindentation. Bone 1999; 25: 295-300. [CrossRef]

16. Rho JY, Ashman RB, Turner CH. Young's modulus of trabecular and cortical bone material: ultrasonic and microtensile measurements. J Biomech 1993; 26: 111-9. [CrossRef]
17. Mason MW, Skedros JG, Bloebaum RD. Evidence of strain-mode-related cortical adaptation in the diaphysis of the horse radius. Bone 1995; 17: 229-37. [CrossRef]
18. Skedros JG, Mendenhall SD, Kiser CJ, Winet H. Interpreting cortical bone adaptation and load history by quantifying osteon morphotypes in circularly polarized light images. Bone 2009; 44: 392-403. [CrossRef]
19. Skedros JG, Sorenson SM, Takano Y, Turner CH. Dissociation of mineral and collagen orientations may differentially adapt compact bone for regional loading environments: results from acoustic velocity measurements in deer calcanei. Bone 2006; 39; 143-51. [CrossRef]
20. Adachi T, Tanaka M, Tomita Y. Uniform stress state in bone structure with residual stress. J Biomech Eng 1998; 120: 342-7. [CrossRef]